

11,12

Anomalous structural transformations of Gd_2O_3 nanopowders obtained in the combustion mode by the glycine-nitrate method

© I.M. Shmytko, V.V. Kedrov

Osipyan Institute of Solid State Physics RAS,
Chernogolovka, Russia

E-mail: shim@issp.ac.ru

Received April 14, 2022

Revised April 14, 2022

Accepted April 19, 2022

The structural states of Gd_2O_3 and $Gd_2O_3:2\%Eu^{3+}$ synthesized by the glycine-nitrate method were studied. As a result of this synthesis, in addition to the known cubic modification of gadolinium oxide, two new previously unknown phases are formed. The first phase is formed during prolonged exposure at room temperature of the initial nanocrystalline cubic structure obtained at a synthesis temperature of $650^\circ C$. The second phase has orthorhombic syngony and is formed during either long-term synthesis at a temperature of $650^\circ C$, or short-term syntheses at a higher temperature. Both phases pass into the traditional cubic modification during further high-temperature annealing. In addition, the effect of structural „infection“ was found, which consists in the fact that during annealing of the cubic phase of Gd_2O_3 doped with Eu^{3+} ions in the range of $800\text{--}1100^\circ C$, its partial transition into the monoclinic phase occurs, which disappears with a further increase in the annealing temperature.

Keywords: synthesis of Gd_2O_3 , glycine-nitrate method, nanocrystalline state, X-ray diffraction research methods, phase transitions.

DOI: 10.21883/PSS.2022.08.54630.351

1. Introduction

Much attention is being paid at present to studying the structural state and phase transformations of nanoscopic systems with change of crystallite size. Simple and complex oxides, as well as fluorides of rare earth elements (REE) are interesting from this viewpoint. Interest in REE oxides and fluorides is first of all due to the fact that many of them have scintillational and luminiferous characteristics. Much attention has been recently paid to rare-earth orthoborate phosphors $ReBO_3$ ($Re = Y, La, Pr, Nd, Sm, Eu, Gd, Tb, Dy$) due to their interesting luminescent properties, such as effective radiation of visible light when exposed to X-ray radiation, vacuum ultraviolet (VUV), standard ultraviolet (UV) or infrared (IR) excitation, [1–11]. These compounds are widely used in color plasma panels and mercury-free fluorescent lamps, [12,13].

We have previously performed detailed structural studies of a number of rare-earth oxide compounds synthesized from the amorphous precursor state, [14–28]. We have demonstrated that their structure greatly depends on crystallite size. Thus, the $LuBO_3$, $Eu_2(MoO_4)_3$, $ScBO_3$ and $TbBO_3$ compounds [14–16], obtained from amorphous precursors, are characterized by cyclic structure rearrangement with increase of crystallite size.

In these compounds, not the phase which is the equilibrium one for the given temperature, but the high-temperature phase is the first to crystallize upon precursor heating. In the course of subsequent annealing accompanied with crystallite growth, this phase first transforms into an

equilibrium low-temperature phase, known for the microcrystalline state, while with further increase of annealing temperature it again transforms into the high-temperature one, but this time an equilibrium one. The main reason for such cyclic structural transformations during synthesis of complex REM oxides was supposed to be the increase of chemical potential due to an increased energy of atoms on the surface of crystallites, the fraction of which increases with size decrease.

The role of surface atoms also clearly manifests itself during compaction of nanopowders of simple REM oxides by formation of additional phases at certain nanocrystallite sizes. These phases disappear during subsequent crystallite growth with increase of annealing temperature, [28].

The effect of structural infection was also recorded, when small additions of doping atoms caused the formation of structures which are typical for oxides of the doping element but do not form in an undoped matrix compound, [20,21,25]. Thus, for instance, small additions of Sc atoms (they form the orthoborate $ScBO_3$ only with the calcite structure) to the YBO_3 amorphous precursor, which has (in the crystalline state) the vaterite hexagonal structure, have caused the formation of YBO_3 in the calcite structure.

The above-mentioned structural effects of simple and complex REM oxides were obtained on the samples synthesized by exchange interaction of nitrates $Re(NO_3)_3$ with boracic acid H_3BO_3 in water medium. Emphasis in the setting of this research is laid on influence of the synthesis method on the original structure and subsequent structural transformations of simple REM oxides with increase of

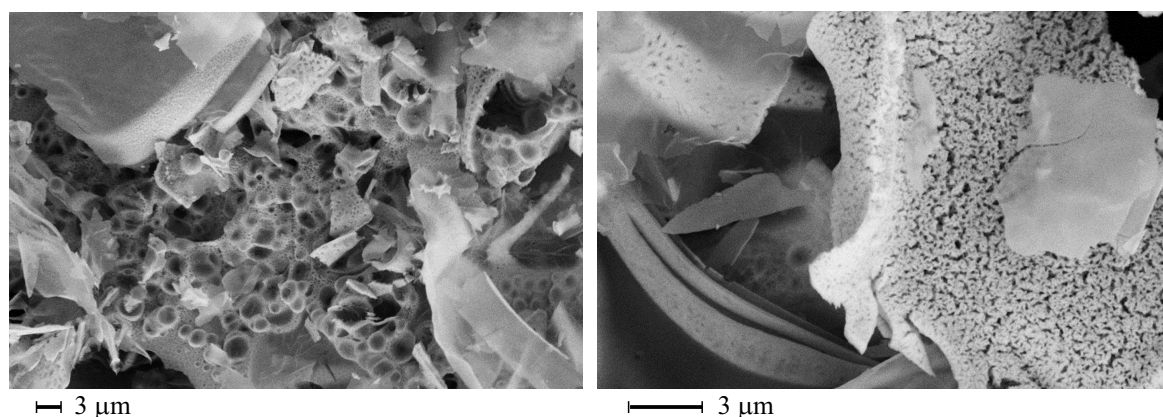


Figure 1. SEM-image of $Gd_2O_3:Eu^{3+}$ powder synthesized at $T = 650^\circ C$ with the synthesis time of 20 min.

annealing temperature. Gadolinium oxide was chosen as the model compound. Gadolinium oxide was chosen as the model compound because it is a good carrier material for luminescent applications, thanks to its thermal, chemical and photochemical stability [29–31]. Gadolinium oxide doped with Eu^{3+} ($Gd_2O_3:Eu^{3+}$) has attractive photoluminescent (PL) properties. It is widely used in fluorescent lamps, television tubes, biological fluorescent labeling [30,32,33], contrast enhancement for MRT [34–36], hyperthermia [37], immunoassays [38,39] and applied applications [40–43]. Gd_2O_3 nanoparticles doped with Eu^{3+} are phosphors with red emission, bright luminescence and long-term photothermal stability [44]. $Gd_2O_3:Eu^{3+}$ are also a very efficient X-ray and thermoluminescent phosphor [45,46].

Gadolinium oxide can be obtained by various methods, such as sol-gel [47], polyol [48], pyrolysis with flame spraying [49,50], laser ablation [51], hydrothermal [42,52,53] and direct deposition [54]. The glycine-nitrate method in the combustion mode was used in this study for gadolinium oxide synthesis. Thereat, since the previous studies did not reflect the peculiarities of the structural states of Gd_2O_3 at the initial synthesis stages, the main task of the present publication is a detailed study of the structural state of gadolinium oxide depending on synthesis time and temperature and subsequent structure transformations during high-temperature annealing of the initially obtained nanocrystalline samples.

2. Samples and experimental procedure

Samples of gadolinium oxide (Gd_2O_3) without doping and with europium atom doping ($Gd_2O_3:2\% Eu^{3+}$) were synthesized for studies. Samples were synthesized in the combustion mode by the glycine-nitrate method, [55,56]. $Gd_2O_3:2\% Eu^{3+}$ was synthesized by adding aqueous solution of europium nitrate in the molar ratio of 98/2 and glycine in the required amount for the process $0.98Gd(NO_3)_3 + 0.02Eu(NO_3)_3 + 1.55C_2H_5NO_2$ (glycine) $\rightarrow 0.5(Gd_{0.98}Eu_{0.02})_2O_3 + 3.11CO_2 + 3.88H_2O$

+ $2.28N_2$ to the aqueous solution of gadolinium nitrate. The glycine amount was taken with a 20% excess from the stoichiometric amount. After water evaporation, a combustion reaction was initiated by placing the precursor into a furnace with the specified synthesis temperature.

A series of 10 samples with different synthesis temperatures and times was obtained. 4 samples of gadolinium oxide were made at the synthesis temperature of $650^\circ C$ and synthesis times of 20 and 100 min: two undoped samples of Gd_2O_3 and two doped samples of $Gd_2O_3:Eu^{3+}$. One sample with the initial synthesis time of 5 min was made at the synthesis temperature of $700^\circ C$ and was additionally annealed at the same temperature for 35 min. Another sample with the short synthesis time of 5 min was made at the synthesis temperature of $800^\circ C$. A sample with the temperature of $850^\circ C$ was made with the same synthesis time. The highest synthesis temperature was equal to $970^\circ C$. The synthesis time in this case was 10 min.

The samples' structural state was recorded at room temperature on a D500 X-ray diffractometer (Siemens) using the Bragg–Brentano scheme. We used CuK_α -radiation monochromated by an output graphite monochromator. Topology of crystallites of the obtained compounds was determined on a SUPRA 50VP scanning electron microscope (SEM). An example of SEM-image of the powder obtained at the synthesis temperature of $650^\circ C$ and synthesis time of 20 min is shown in Fig. 1.

Temperature annealing was performed in a SNOL-6.7/1300 laboratory furnace in air for 1.5–2 h at each temperature point. Thereat, the temperature interval between subsequent annealing operations was $25\text{--}100^\circ C$ depending on the observed spectrum changes after the previous annealing.

The experiments were conducted in two stages. The first stage included synthesis of samples and their structural modification with additional high-temperature annealing. The second stage was performed after a prolonged keeping (almost in one year) of samples at room temperature. At this stage we performed a repeated detailed identification of all samples and studied the structural deformations of

all samples during subsequent successive high-temperature annealing.

3. Experimental results and discussion

Fig. 2 shows the X-ray diffraction spectra of the initial state of the synthesized $\text{Gd}_2\text{O}_3:2\%\text{Eu}^{3+}$ samples. Spectrum *a* in Fig. 2 pertains to the sample obtained at the minimum synthesis temperature of 650°C for 20 min. According to the PDF-2 database, this spectrum is typical for the cubic Gd_2O_3 structure with a space group of symmetry *S.G.Ia-3*. The wide pattern of the diffraction lines characterizes the sample state as nanocrystalline. The size of *D* crystallites calculated using the Scherrer formula $\beta = \lambda/D \cos\theta$, where β is reflection width at half the reflection height, λ — used radiation wavelength, θ — diffraction angle for the given reflection, is estimated as follows: $\langle D \rangle \approx 120 \text{ \AA}$. An increase of synthesis time at 650°C to 100 min and shorter synthesis of samples ($t \leq 10 \text{ min}$) at higher temperatures have resulted in the formation of a two-phase state from a new unknown phase (called phase-1) and residues of the Gd_2O_3 cubic phase. The spectra *b, c, d, e* in Fig. 2 show that the cubic phase is in the nano-state, while the new phase-1 is characterized by narrower reflections, which indicates a larger size of nanocrystallites. The estimates show that both the sizes of the known cubic phase and the sizes of the crystallites of phase-1 increase with temperature rise. Thus, the ratio of sizes of crystallites of both phases for the sample obtained at 650°C and 100 min of synthesis are equal to $D_{\text{cub}}/D_{\text{new}} = 214/280 \text{ \AA}$, and for the sample synthesized at 970°C and 10 min. this ratio is equal to $D_{\text{cub}}/D_{\text{new}} = 412/616 \text{ \AA}$ respectively.

The situation changed completely after keeping of all the original samples at room temperature for \sim a year. Fig. 3 shows the spectra of the same samples as in Fig. 2 after keeping for a year. A comparison of the spectra in Fig. 2 and 3 indicates their three differences. The first, more noticeable, difference is in the almost complete disappearance of the cubic phase. Its residues are more or less noticeable for the sample obtained at the synthesis temperature of 970°C . At the same time, the positions of the reflections of the new phase-1 are completely retained and have a higher intensity. This means that the energy of phase-1 formation is below the energy of formation of an equilibrium cubic modification Gd_2O_3 . We determined the crystalline syngony of phase-1 using the POWD software and obtained the maximum matching of the positions of all strong reflections with an orthorhombic lattice having the cell parameters $a = 5.5892$, $b = 6.6664$, $c = 5.5833 \text{ \AA}$, $V = 208.03 \text{ \AA}^3$. Fig. 4 shows the spectrum of this orthorhombic phase with indices of the strongest reflections at room temperature.

The second noticeable change is the complete disappearance of the cubic phase reflections for the sample, synthesized at 650°C and synthesis time of 20 min, and appearance of reflections of a new unknown nanocrystalline

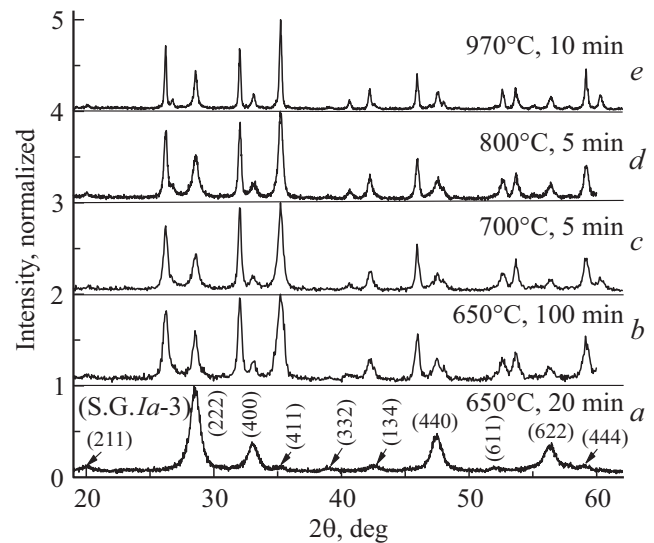


Figure 2. Diffraction spectra of the initial state of the synthesized $\text{Gd}_2\text{O}_3:2\%\text{Eu}^{3+}$ samples. *a* — synthesis temperature 650°C , synthesis time 20 min. *b* — synthesis temperature 650°C , synthesis time 100 min. *c* — synthesis temperature 700°C , synthesis time 5 min. *d* — synthesis temperature 800°C , synthesis time 5 min. *e* — synthesis temperature 970°C , synthesis time 10 min.

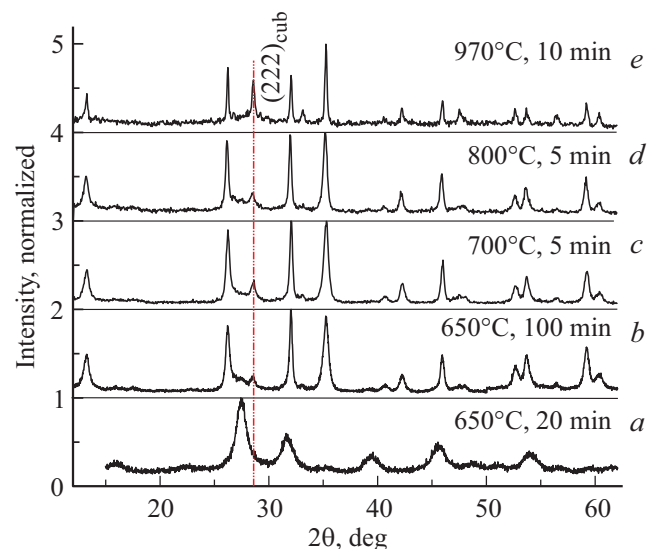


Figure 3. Diffraction spectra of the structural state of the synthesized $\text{Gd}_2\text{O}_3:2\%\text{Eu}^{3+}$ samples after keeping at room temperature for a year. *a* — synthesis temperature 650°C , synthesis time 20 min. *b* — synthesis temperature 650°C , synthesis time 100 min. *c* — synthesis temperature 700°C , synthesis time 5 min. *d* — synthesis temperature 800°C , synthesis time 5 min. *e* — synthesis temperature 970°C , synthesis time 10 min.

phase (phase-2). This is illustrated in Fig. 5. It can be seen that the strongest reflections of the new phase-2 sort of repeat the strong reflections of the original cubic phase and are slightly offset to the region of smaller diffraction angles. This means that the crystalline cell of phase-2

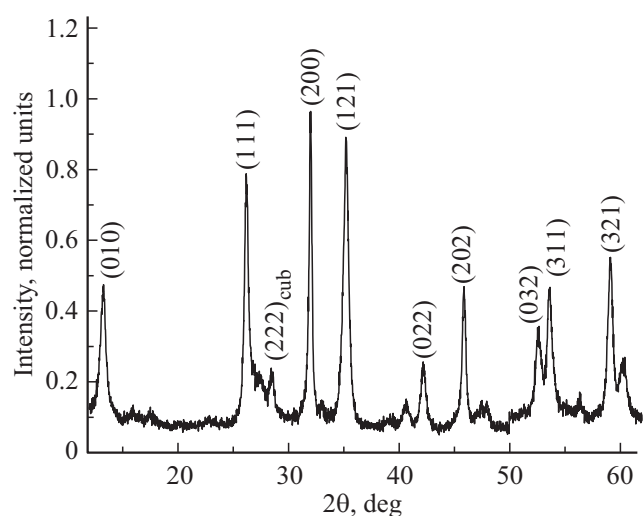


Figure 4. Diffraction spectrum of the $Gd_2O_3:2\%Eu^{3+}$ sample obtained at the synthesis temperature of $650^\circ C$ and synthesis time of 100 min, after long-term keeping at room temperature.

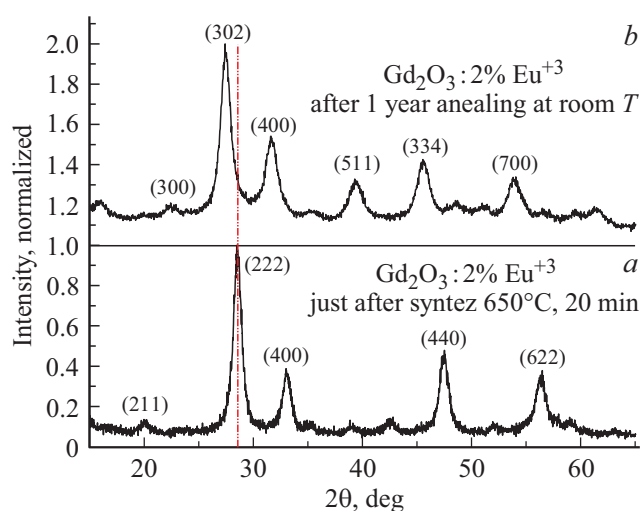


Figure 5. Diffraction spectra of the structural state of the synthesized $Gd_2O_3:2\%Eu^{3+}$ sample obtained at the synthesis temperature of $650^\circ C$ and synthesis time of 20 min. *a* — right after synthesis; *b* — after a year.

does not greatly differ in volume from the cubic one, while presence of additional reflections means a decrease of the symmetry of the new phase-2 to pseudo-cubic. The POWD software was used to establish syngony and cell parameters of phase-2: syngony is tetragonal, lattice parameters are $a = 11.900 \text{ \AA}$, $b = 11.307 \text{ \AA}$, $V = 1601 \text{ \AA}^3$.

Phase-2 is thermodynamically equilibrium. Subsequent successive stepped annealing of the sample to $400^\circ C$ has resulted in a complete transition of the tetragonal phase-2 to the original nanocrystalline cubic phase Gd_2O_3 , see spectrum *d* in Fig. 6. Thereat, a smooth transformation of the spectra of the tetragonal phase-2 into the original cubic phase formed during synthesis, is clearly seen. It

should be noted that the subsequent increase of annealing temperature did not cause a transition of the recovered cubic phase into the new phase-1 shown in spectra *b, c, d, e* in Fig. 3. With increase of annealing temperature above $400^\circ C$, only the half-width of the cubic phase reflections decreased, see the spectrum *e* in Fig. 6, which shows the natural nanocrystallite growth with increase of annealing temperature. This means that the orthorhombic phase-1 is non-equilibrium and kinetics of its phase formation in the suggested method of gadolinium oxide synthesis depends on synthesis temperature and time.

It is obvious that at this stage we do not know the space group of symmetry both of the tetragonal phase for synthesis at $650^\circ C$ for 20 min and the space group of symmetry for the orthorhombic phase. Additional research will be dedicated to this issue.

Evolution of the orthorhombic phase during subsequent high-temperature annealing was studied. The transformation of the spectra of this phase by the example of the sample, synthesized at $650^\circ C$ for 100 min., is shown in Fig. 7. It is clearly seen that the orthorhombic phase-1 during high-temperature annealing transforms into the known cubic phase Gd_2O_3 , into which it finally transforms at the annealing temperature of $725^\circ C$.

An interesting phenomenon was found by the example of the sample synthesized at $T = 850^\circ C$ for 5 min. The essence of this phenomenon is shown in Fig. 8. At first, weak reflections of the high-temperature monoclinic modification Gd_2O_3 appeared in the diffraction spectrum in case of sample annealing at $800^\circ C$ for 6 h; with subsequent increase of annealing temperature, these reflections became more intense (see spectrum *b*), and then they began disappearing and disappeared completely during annealing at $1100^\circ C$ for 8.5 h.

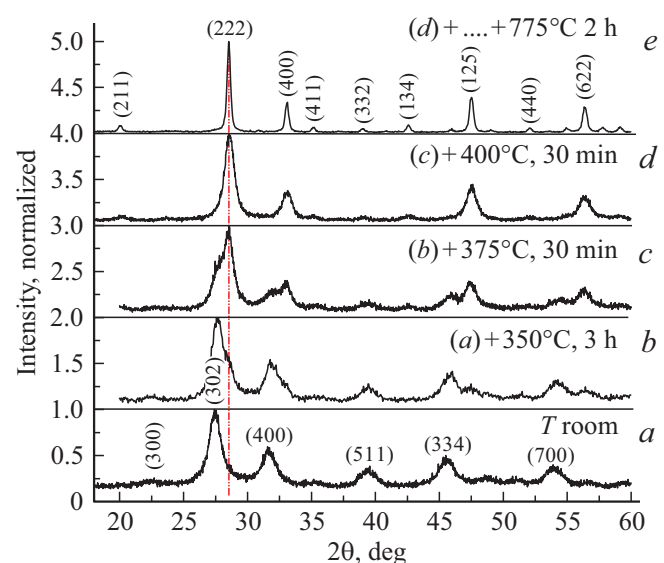


Figure 6. Temperature change of the diffraction spectra of the $Gd_2O_3:2\%Eu^{3+}$ sample, synthesized at $650^\circ C$ and synthesis time of 20 min, a year after synthesis. The annealing characteristics are shown in the figure.

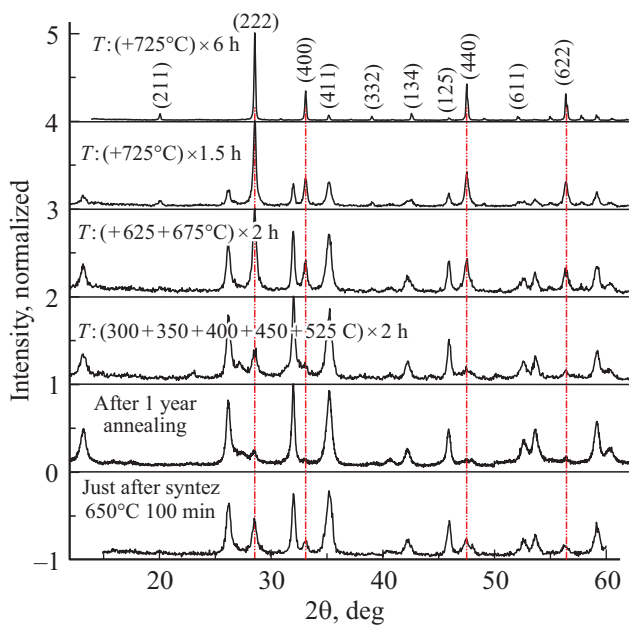


Figure 7. Transformation of the diffraction spectrum of the orthorhombic phase into a cubic one during successive annealing operations.

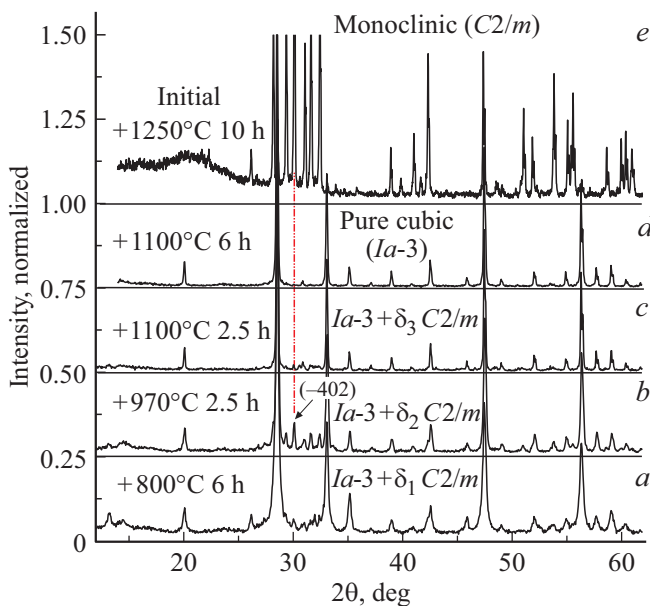


Figure 8. Temperature change of the diffraction spectra of the cubic phase sample $\text{Gd}_2\text{O}_3:2\% \text{Eu}^{3+}$ during sample annealing in the range of 800–1250°C.

The obtained result can be interpreted as follows. It is known that the temperature of transition from the Gd_2O_3 cubic structure into the monoclinic phase for micropowders is equal to $\approx 1600^\circ\text{C}$. At the same time, the transition from the cubic phase into the monoclinic phase for Eu_2O_3 for the microcrystalline state of the powder is in the range of 1050–1100°C [57]. It would seem that the recorded reflections can be a reflection of the monoclinic modification

of Eu_2O_3 , but this is not so due to two reasons. The first reason is that the position of the reflections does not match the position of the reflections of the europium oxide monoclinic modification, but matches the position of the reflections of the Gd_2O_3 monoclinic phase. The second reason is the fact that sample doping with europium did not exceed 2%, while the maximum peak intensity of the reflection (–402) of monoclinic phase emissions at the annealing temperature of 970°C, is $\approx 10\%$ from the maximum peak intensity of cubic phase reflection (222). The obtained result can be interpreted as a structural infection of local regions of the surrounding Gd_2O_3 matrix with Eu^{3+} ions, which results in the formation of a monoclinic modification of gadolinium oxide in them. The question arises: „Why do the formed inclusions of the monoclinic phase disperse with subsequent increase of annealing temperature“. The possible reason for „dispersion“ can be a heterogeneous distribution of doping Eu atoms across the matrix during synthesis. In this case, a certain excess of doping atoms may form in certain regions; the concentration of such atoms is sufficient for „structural infection“ of these matrix areas with the monoclinic phase. Further increase of annealing temperature results in a larger amplitude of atom vibrations, which corresponds to an increase of the diffusion coefficient and, consequently, to a more uniform distribution of doping atoms across the matrix, which causes disappearance of the monoclinic inclusions.

The final transition of the cubic phase to the monoclinic modification was recorded upon annealing temperature increase to 1250°C and annealing time of 10 h, which is shown in spectrum *e* in Fig. 8. The SEM-image of the crystallites of the obtained monoclinic modification is shown in Fig. 9.

The results given above pertained to gadolinium oxide Gd_2O_3 doped with 2% of europium. Two types of „pure“ samples were synthesized to check the impact of doping on the phase states of Gd_2O_3 . The synthesis parameters for the first sample type: $T = 650^\circ\text{C}$, synthesis time 20 min. The synthesis parameters for the second sample type: $T = 650^\circ\text{C}$, synthesis time 100 min. The diffraction spectrum of the second sample type fully matched the spectrum of the $\text{Gd}_2\text{O}_3:\text{Eu}^{3+}$ samples synthesized at $T = 650^\circ\text{C}$ and synthesis time of 100 min. It also reflected the two-phase state from the conventional cubic phase and the new orthorhombic phase.

The spectrum of the Gd_2O_3 sample with the synthesis time of 20 min differed from the spectrum of the cubic phase of the $\text{Gd}_2\text{O}_3:\text{Eu}^{3+}$ sample synthesized at $T = 650^\circ\text{C}$ and synthesis time of 20 min, see Fig. 10 spectrum *b* (compare with spectrum *a* in Fig. 2). The reflections in spectrum *b* are split into two components. To reveal the nature of this two-component spectrum, Fig. 10 shows spectrum *a* of the $\text{Gd}_2\text{O}_3:\text{Eu}^{3+}$ sample after long-term keeping at room temperature and spectrum *c* of the Gd_2O_3 sample after one-hour annealing at 650°C. A comparison of all three spectrum illustrates that the two-component spectrum is a sum of the spectra of the tetragonal and cubic

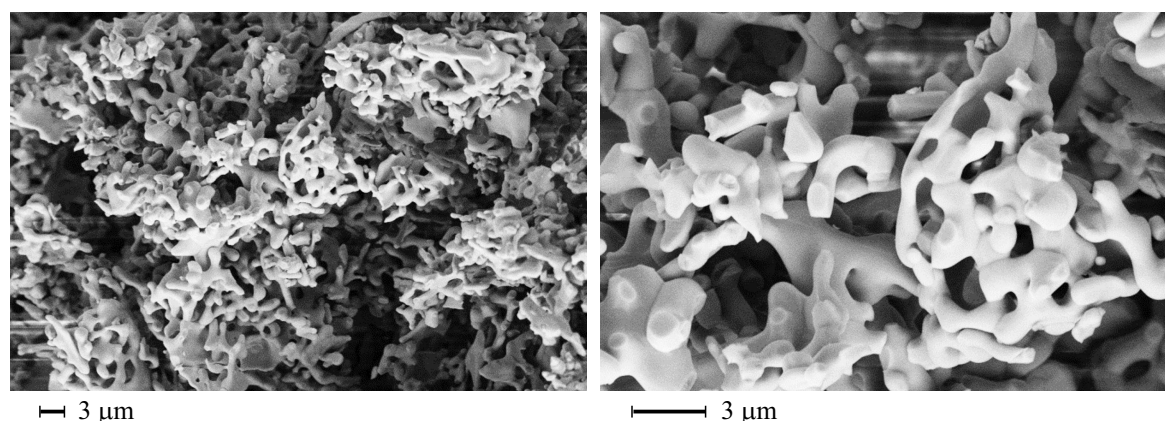


Figure 9. SEM-image of the $Gd_2O_3:Eu^{3+}$ powder annealed at $T = 1250^\circ C$ for 10 h.

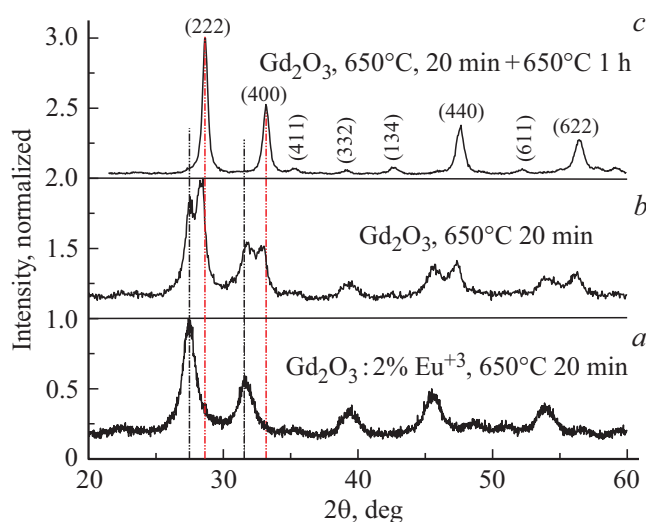


Figure 10. Diffraction spectra of the $Gd_2O_3:2\% Eu^{3+}$ sample obtained at the synthesis temperature of $650^\circ C$ and synthesis time of 20 min, after long-term keeping at room temperature (a), and the Gd_2O_3 sample obtained at the same conditioned right after synthesis (b). c — spectrum of the sample represented by spectrum (b), after annealing at $650^\circ C$ for 1 hour.

phases. Thus, we may state that new previously unknown tetragonal and orthorhombic phases exist both for the simple and doped gadolinium oxide Gd_2O_3 . The tetragonal phase precedes the formation of the known cubic modification is the lowest-temperature one.

The natural question arises: „Why were these phases not recorded previously with other synthesis methods“. Attention here should be paid to the crystallite size during synthesis by the glycine-nitrate method. As stated above, the size of cubic modification crystallites was ≈ 12 nm. With this crystallite size, the fraction of surface atoms is very large, which will considerably affect the chemical potential of the whole system. The latter, in our opinion, determines the thermodynamic conditions of origination of new, previously unknown phase states of Gd_2O_3 .

4. Conclusion

Summing up the obtained results, let us note the main ones. As we have supposed in the setting of this research, the structural states of simple oxides of rare earth elements depend greatly on synthesis method. By the example of synthesis of Gd_2O_3 and $Gd_2O_3:Eu^{3+}$, new structural states have been obtained in the combustion mode by the glycine-nitrate method; these states depend on synthesis temperature and time. We have discovered a new nanocrystalline tetragonal phase which forms at the first stages of crystal formation. It has turned out that both the conventional cubic structure and a two-phase state can be obtained from the cubic modification Gd_2O_3 and the new orthorhombic structure at low synthesis temperatures, depending on synthesis duration. Thereat, subsequent annealing of this structure in air causes its transformation into the cubic modification.

We would like to expressly indicate the revealed effect of structural infection of Gd_2O_3 with doping element atoms (Eu); during medium-temperature annealing this causes the formation of monoclinic regions in the cubic matrix, which disperse with increase of annealing temperature.

Acknowledgments

The authors would like to sincerely thank E.Yu. Postnova for the SEM-analysis of the synthesized $Gd_2O_3:Eu^{3+}$ samples at different stages of their heat treatment.

Funding

The work has been performed under the state assignment of ISSP of RAS.

Conflict of interest

The authors declare that they have no conflict of interest.

References

- [1] Z. Wei, L. Sun, C. Liao, J. Yin, X. Jiang, C. Yan, S. Lü. *J. Phys. Chem. B* **106**, 22, 10610 (2002).
- [2] H. Giesber, J. Ballato, W. Pennington, J. Kolis. *J. Inf. Sci.* **149**, 1–3, 61 (2003).
- [3] H. Giesber, J. Ballato, G. Chumanov, J. Kolis, M. Dejneka. *J. Appl. Phys.* **93**, 11, 8987 (2003).
- [4] T. Kim, S. Kang. *Mater. Res. Bull.* **40**, 11, 1945 (2005).
- [5] J. Lin, Y. Huang, J. Zhang, X. Ding, S. Qi, C. Tang. *Mater. Lett.* **61**, 7, 1596 (2007).
- [6] L. Chen, Y. Jiang, S. Chen, G. Zhang, C. Wang, G. Li. *J. Lumin.* **128**, 12, 2048 (2008).
- [7] J. Dexpert-Ghys, R. Mauricot, B. Caillier, P. Guillot, T. Beaudette, G. Jia, P. Tanner, B. Cheng. *J. Phys. Chem. C* **114**, 14, 6681 (2010).
- [8] J. Li, Y. Wang, B. Liu. *J. Lumin.* **130**, 7, 981 (2010).
- [9] A. Szczeszak, S. Lis, V. Nagirnyi. *J. Rare Earths* **29**, 12, 1142 (2011).
- [10] Z. Yang, D. Yan, K. Zhu, Z. Song, X. Yu, D. Zhou, Z. Yin. *J. Mater. Lett.* **65**, 8, 1245 (2011).
- [11] A. Szczeszak, T. Grzyb, S. Lis, R. Wiglusz. *J. Dalton Trans.* **41**, 19, 5824 (2012).
- [12] S. Choi, B.-Y. Park, H.-K. Jung. *J. Lumin.* **131**, 7, 1460 (2011).
- [13] C.R. Ronda, T. Jüstel, H. Nikol. *J. Alloys Compd.* **275–277**, 669 (1998).
- [14] I.M. Shmytko, G.K. Strukova, E.A. Kudrenko. *Crystallogr. Rep.* **51**, Suppl. 1, S163 (2006).
- [15] I.M. Shmytko. *FTT* **61**, 2, 340 (2019) (in Russian).
- [16] I.M. Shmytko. *FTT* **61**, 11, 2210 (2019) (in Russian).
- [17] E.A. Kudrenko, I.M. Shmytko, G.K. Strukova. *FTT* **50**, 5, 924 (2008) (in Russian).
- [18] I.M. Shmytko, E.A. Kudrenko, G.K. Strukova, N.V. Klassen. *FTT* **50**, 6, 1108 (2008) (in Russian).
- [19] I.M. Shmytko, E.A. Kudrenko, G.K. Strukova. *FTT* **51**, 9, 1834 (2009) (in Russian).
- [20] I. Shmytko, G. Strukova, E. Kudrenko. *Acta Cryst. A* **66**, S230 (2010).
- [21] I.M. Shmytko, I.N. Kiryakin, G.K. Strukova. *FTT* **53**, 2, 353 (2011) (in Russian).
- [22] I. Shmytko. *Acta Cryst. A* **67**, S533 (2011).
- [23] V.V. Kedrov, I.M. Shmytko, S.Z. Shmurak, E.A. Kudrenko, N.V. Klassen. *J. Mater. Res.* **27**, 16, 2117 (2012).
- [24] I.M. Shmytko, I.N. Kiryakin, G.K. Strukova. *FTT* **55**, 7, 1364 (2013) (in Russian); *FTT* **55**, 7, 1369 (2013) (in Russian).
- [25] E.A. Kudrenko, I.M. Shmytko, G.K. Strukova. *FTT* **50**, 5, 924 (2008) (in Russian).
- [26] E.A. Kudrenko, I.M. Shmytko, G.K. Strukova. *Acta Cryst., A* **64**, S427 (2008).
- [27] I.M. Shmytko, E.A. Kudrenko, G.K. Strukova, V.V. Kedrov, N.V. Klassen. *Z. Kristallogr. Suppl.* **27**, 211 (2008).
- [28] I.M. Shmytko, G.R. Ganeeva, A.S. Aronin. *FTT* **57**, 1, 129 (2015) (in Russian).
- [29] Y. Zhou, J. Lin, S. Wang. *J. Solid State Chem.* **171**, 1, 391 (2003).
- [30] H. Lu, G. Yi, S. Zhao, D. Chen, L. Guo, H. Cheng. *J. Mater. Chem.* **14**, 1336 (2004).
- [31] T. Hirai, T. Orikoshi. *J. Colloid Interface Sci.* **269**, 1, 103 (2004).
- [32] J.N. Anker, R. Kopelman. *Appl. Phys. Lett.* **82**, 7, 1102 (2003).
- [33] S. Lechevallier, P. Lecante, R. Mauricot, H. Dexpert, J. Dexpert-Ghys, H. Kong, H.K. Kong, G.L. Law, K.L. Wong. *Chem. Mater.* **22**, 22, 6153 (2010).
- [34] J.E. Lee, N. Lee, H. Kim, J. Kim, S.H. Choi, J.H. Kim, T. Kim, I.C. Song, S.P. Park, W.K. Moon, T. Hyeon. *J. Am. Chem. Soc.* **132**, 2, 552 (2010).
- [35] X. Wenlong, Y.P. Ja, K. Krishna, A.B. Badrul, C.H. Woo, J. Seonguk, W.P. Jang, Ch. Yongmin, Y.D. Ji, S.Ch. Kwon, J.K. Tae, A.P. Ji, W.K. Young, H.L. Gang. *New J. Chem.* **36**, 11, 2361 (2012).
- [36] G. Liu, G. Hong, J. Wang, X. Dong. *J. Alloys Compd.* **432**, 1–2, 200 (2007).
- [37] M. Johannsen, U. Gneveckow, L. Eckelt, A. Feussner, N. Waldofner, R. Scholz, S. Deger, P. Wust, S. Loening, A. Jordan. *Int. J. Hyperthermia* **21**, 7, 637 (2005).
- [38] J. Feng, G. Shan, A. Maquieira, M.E. Koivunen, B. Guo, B.D. Hammock, I.M. Kennedy. *An. Chem.* **75**, 19, 5282 (2003).
- [39] M. Níchkova, D. Dosev, S.J. Gee, B.D. Hammock, I.M. Kennedy. *An. Chem.* **77**, 21, 6864 (2005).
- [40] G. Blasse, B.C. Grabmaier. *Luminescent materials / Eds G. Blasse, B.C. Grabmaier. Springer, Berlin (1994). 232 p.*
- [41] W. Rossner. *IEEE Trans. Nucl. Sci.* **40**, 4, 376 (1993).
- [42] E.M. Goldys, K. D-Tomsia, S. Jinjun, D. Dosev, I.M. Kennedy, S. Yatsunenko, M. Godlewski. *J. Am. Chem. Soc.* **128**, 45, 14498 (2006).
- [43] V. Bedekar, D.P. Dulta, M. Mohapatra, S.V. Godbole, R. Ghildiyal, A.K. Tyagi. *Nanotechnology* **20**, 12, 5707 (2009).
- [44] R.N. Bhargava. *J. Lumin.* **70**, 1–6, 85 (1996).
- [45] W. Rossner, B.C. Grabmaier. *J. Lumin.* **48–49**, 1, 29 (1991).
- [46] F. Jintai, Y. Xinqiang, L. Rihong, D. Hongxing, W. Jun, Z. Long. *Opt Lett.* **36**, 11, 4347 (2011).
- [47] A.G. Murillo, A.M. Ramírez, F.C. Romo, M.G. Hernández, M.D. Crespo. *Mater Lett.* **04**, 7, 034 (2009).
- [48] A. Müller, O. Heim, M. Panneerselvam, M. Willert-Porada. *Res. Bull.* **40**, 12, 2153 (2005).
- [49] F. Mangiarini, R. Naccache, A. Speghini, M. Bettinelli, F. Vetrone, J.A. Capobianco. *Mater. Res. Bull.* **45**, 8, 927 (2010).
- [50] Y. Iwako, Y. Akimoto, M. Omiya, T. Ueda, T. Yokomori. *J. Lumin.* **130**, 8, 1470 (2010).
- [51] G. Ledoux, D. Aman, C. Dujardin, K. Masenelli-Varlot. *Nanotechnology* **20**, 44, 445605 (2009).
- [52] G. Liu, G. Hong, J. Wang, X. Dong. *J. Alloys Compd.* **432**, 1–2, 200 (2007).
- [53] Kyung-Hee Lee, Yun-Jeong Bae, Song-Ho Bayeon. *Bull. Korean Chem. Soc.* **29**, 11, 2161 (2008).
- [54] R. Bazzia, M.A. Flores-Gonzalez, C. Louisa, K. Lebboua, C. Dujardina, A. Breniera, W. Zhanga, O. Tillementa, E. Bernstein, P. Perriat. *J. Lumin.* **102**, 5, 445 (2003).
- [55] K.C. Patil, T. Mimani, S.T. Aruna. *Current Opinion Solid State Mater. Science* **6**, 6, 507 (2002).
- [56] K.C. Patil, M.S. Hegde, T. Rattan, S.T. Aruna. *Chemistry of Nanocrystalline Oxide Materials: Combustion Synthesis, Properties and Applications. World Scientific, New Jersey (2008). 364 p.*
- [57] R.G. Haire, L. Eyring. *Handbook Phys. Chem. Rare Earths* **18**, 413 (1994).